Journal of Catalysis **191,** 282–293 (2000)
doi:10.1006/jcat.2000.2819, available online at http://www.idealibrary.com on IDEAL®

# The Controlled Oxidation of Hydrogen from an Explosive Mixture of Gases Using a Microstructured Reactor/Heat Exchanger and $Pt/Al_2O_3$ Catalyst

Michael T. Janicke,* Harry Kestenbaum,* Ulrike Hagendorf,* Ferdi Schüth,*,[1]
Maximilian Fichtner,† and Klaus Schubert†

*Max Planck Institut für Kohlenforschung, Kaiser-Wilhelm-Platz 1, D-45470 Mülheim an der Ruhr, Germany; and †Forschungszentrum Karlsruhe GmbH, Postfach 3640, D-76021 Karlsruhe, Germany

Received June 7, 1999; revised December 13, 1999; accepted January 6, 2000

DEDICATED TO PROF. D. HÖNICKE ON THE OCCASION OF HIS 60TH BIRTHDAY.

**With advances achieved in the area of microreactor technology, new possibilities for the use of microchannel reactors in the field of heterogeneous catalysis are now attainable. By exploiting these microstructured reactors for their relatively high surface-to-volume ratio and the inherent safety due to dimensions below the quenching distance at which explosions can propagate, hazardous reaction mixtures can be handled safely. The aim of this paper is to present the results on the catalytic $H_2/O_2$ reaction obtained from an alumina-coated microstructured reactor/heat exchanger that has been impregnated with a platinum catalyst. With this reactor, explosive mixtures of gaseous hydrogen and oxygen (up to 50% by volume of $H_2$ in $O_2$) were safely handled and the hydrogen was completely converted to water without explosions by maintaining a heterogeneously catalyzed reaction. The homogeneous reaction was prevented through efficient removal of the heat evolved from this highly exothermic reaction with cooling gas flowing in the heat exchanger channels of the reactor. It is anticipated that the use of microstructured reactors in catalysis research will add new levels of safety and control in studying chemical systems that necessarily involve explosive mixtures of gases.** 

*Key Words:* **microstructured reactor; $H_2/O_2$ reaction; Pt catalyst; $Al_2O_2$ support.**

## INTRODUCTION

In recent years, the field of microreaction technology has emerged as an area of interest for reaction engineering studies and chemical industries (1–3). Much consideration has been paid to microstructured reactors, also known as microchannel reactors, because of distinct advantages they provide over conventional reactor design. Microstructured reactors' benefits include their inherent safety, improved process control, and rapid implementation. The small size of the microchannels translates to smaller concentrations of dangerous chemicals and the microstructured features result in reactor dimensions that are less than the quench distances for explosions, ultimately providing an opportunity to produce hazardous chemicals on-site safely and in a cost-effective manner that eliminates the need to transport these species (4–7). Improved process control can be realized because of fast response times in the microstructured reactors (4). These improved response times arise from high surface-to-volume ratios that lead to efficient heat and mass transfer, for example. Additionally, microreactors can be designed to provide rapid mixing in the micron-sized channels, a further advantage when enhanced process control and response times are required. Lastly, microreactor technology is supposed to be quickly transferred from laboratory or pilot plant stages to production facilities because the microstructures with quasi-identical reaction channels can be scaled up to achieve throughputs in the range of 100,000 t/year of liquids with one or a few devices (8).

There are many examples of chemical reactions that are well suited for microreactors. A brief list of possibilities includes partial oxidation reactions in which kinetically fast reactions must be quenched to prevent full oxidation (8–11), multiphase reactions that are mass transfer limited but require effective mixing (5), reactions that are highly exothermic or involve explosive mixtures such as the $H_2/O_2$ reaction (5, 12, 13), and finally reactions that involve toxic precursors or products (hydrogen cyanide or phosgene are two plausible candidates) (6, 7). Of these, the $H_2/O_2$ reaction is a particularly demanding test case in that the reaction is extremely exothermic and nearly all mixtures of $H_2$ in $O_2$ gases are explosive. For these reasons, the $H_2/O_2$ reaction over a $Pt/Al_2O_3$ catalyst was selected for this research in an effort to demonstrate the strength of microreactors in safely handling hazardous chemical reactions. Whereas this work focuses on the reaction of hydrogen and oxygen on a platinum catalyst, much broader opportunities have been realized in other areas of oxidation chemistry

[1] To whom correspondence should be addressed. E-mail: schueth@mpi-muelheim.mpg.de. Fax: +49 (0) 208 306-2995.



0021-9517/00 $35.00

which also rely on explosive mixtures of hydrogen and oxygen (5).

The precarious nature of the hydrogen/oxygen reaction is a consequence of the exothermicity and the broad explosion limits for $H_2$; however, the challenges this system presents are solved by using a microstructured reactor/heat exchanger. For the $H_2/O_2$ reaction,

$$H_{2(g)} + \tfrac{1}{2}O_{2(g)} \rightarrow H_2O_{(g)} \quad \Delta H = -57.9\,\text{kcal/mol}$$

with the explosion limits for $H_2$ in $O_2$ ranging from 4% to 94%, on a volume percent basis, and from 4% to 75% for $H_2$ in air (14), the safety issues cannot be overstressed and expensive equipment and reactors are normally required to handle the reaction. Microstructured reactors provide many advantages over conventional reactor designs, as is shown in this work with a stainless steel microstructured reactor/heat exchanger. The small reactor minimizes the explosion danger by possessing a small reactor volume, ca. 1 $cm^3$, and the dimensions of the microchannels ($140 \times 200\ \mu$m) are smaller than the quenching distance for hydrogen, the critical distance below which no flame can propagate. For hydrogen in a capillary tube, the quench distance has been reported to be 1000 $\mu$m (15), 5 times greater than the largest dimension of the micromachined channels of the reactor used in this study. Heat evolved from the reaction is removed from the reactor system by a second set of perpendicular channels, providing a means to control the temperature of the reactor with cooling gas. In combination, micron-sized channels and efficient heat removal minimize the explosion hazard.

The motivation for this project with the $Al_2O_3$/Pt-coated microreactor is to demonstrate the additional feasibility of microreactor technology in the development of fuel cell components that are suitable for vehicles. With the current push to limit the global $CO_2$ emissions (16), much attention has been focused on more efficient means of transportation that produce lower carbon emissions. One part in decreasing the amount of $CO_2$ can be achieved by replacing internal combustion engines that depend on fossil fuels with environmentally friendly fuel cells. The practical development of an electric propulsion system based on proton-exchange membrane fuel cells which utilize advances in microreactor technology has been previously addressed (11, 17). In particular, Peters and co-workers have shown that through the use of a microreactor system for the steam-reforming of methanol at temperatures obtainable with this reactor (ca. 280°C), the goal of a lightweight fuel cell for powering an electric motor, competitive with the internal combustion engine, can be realized (17, 18). The work presented here will describe one component of this system, a catalytic burner that could be used to convert hydrogen off-gas from a fuel cell to the heat required to drive a steam reformer, expanding upon results previously presented (12).

## EXPERIMENTAL

### 1. *Microstructured Reactor/Heat Exchanger*

The microstructured reactor/heat exchanger used for this work, shown in Fig. 1, was designed and built by the Karlsruhe Research Center *(Forschungszentrum Karlsruhe GmbH)* (1, 19). The reactor is assembled from individual stainless steel plates with micromachined channels. When the plates are stacked one on top of the other with a 90° rotation between each plate, two sets of perpendicular channels are produced. The stack of plates is diffusion bonded together, resulting in an essentially monolithic stainless steel assembly whose channels are vacuum tight and can also handle high pressures (1, 19). A stainless steel housing with standard tube connections is welded onto the assembly to complete the reactor. For this particular reactor, two sets of foils with differently sized channels were used. The set of larger channels ($140 \times 200\ \mu$m), coated with $Al_2O_3$ and impregnated with Pt, are used for the $H_2/O_2$ reaction while the smaller channels ($70 \times 100\ \mu$m) function as a heat exchanger.

### 2. *Alumina Deposition*

The stainless steel microreactor/heat exchanger was coated with alumina to increase the overall surface area of the microchannels and to protect the surface from reacting electrochemically with the hexachloroplatinic acid precursor solution necessary for the Pt catalyst. The $Al_2O_3$ layer was grown on the reactor channels by an atmospheric CVD process utilizing aluminum isopropoxide, $Al[(CH_3)_2CHO]_3$, as the alumina precursor. The use of aluminum isopropoxide, $Al(O^iPr)_3$, for the production of aluminum oxide coatings has been described previously (20, 21) and for this work an experimental procedure similar to the earlier work by Aboaf was followed (22). Molten $Al(O^iPr)_3$ (m.p. 140°C) was kept at a constant temperature of 160°C in a glass bubbler through which 1.0 L/min of $N_2$ was passed. This $N_2/Al(O^iPr)_3$ was mixed with $O_2$ flowing at 7.0 L/min. Oxygen was necessary for the decomposition of the alkoxide and to prevent the buildup of carbon in the reactor. Following mixing, the combination of gases passed through the larger $140 \times 200\ \mu$m channels in the reactor at 300°C for 1 h, heated to 300°C by passing 7 L/min of preheated $N_2$ through the set of smaller microchannels ($100 \times 70\ \mu$m). Additional heating could be obtained by placing external cartridge heaters in aluminum blocks above and below the reactor. Ceramic cloth was used to insulate the reactor and maintain the elevated temperature. After 1 h, the reactor was cooled, and the flow direction was reversed for a second 1-h period so that the entrance and exit of the reactor would have similar alumina coatings. Note the coating system had to be operated for extended periods of time to work reliably. It was found

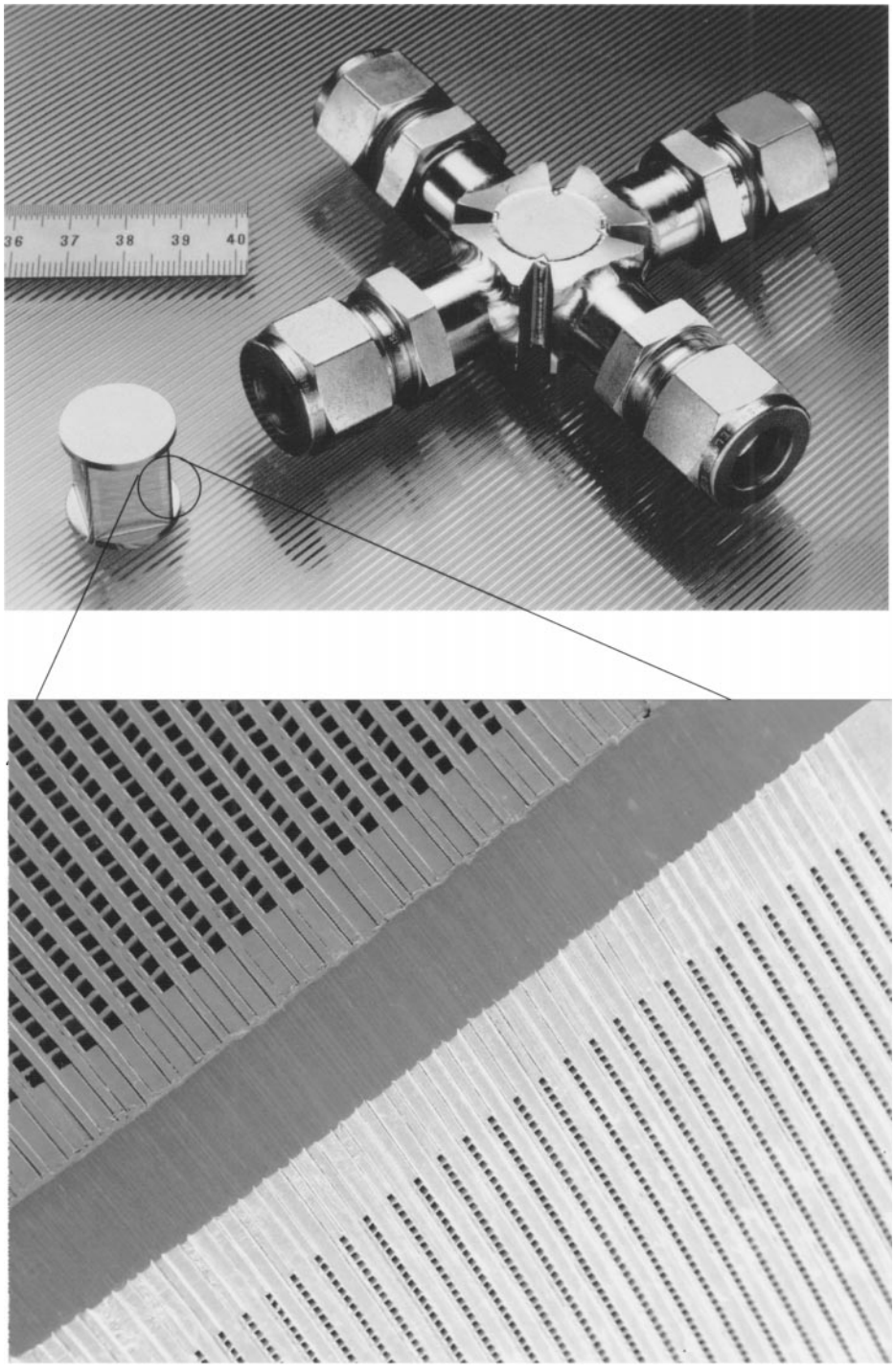


**FIG. 1.** Photographs of the microstructured reactor developed and constructed by the Karlsruhe Research Center. Above is shown the reactor with and without the attached pipe fittings. A ruler in centimeters is included to show the scale. The bottom picture is a SEM micrograph showing a corner view of the reactor. The larger channels ($140 \times 200\ \mu$m) appear to be going into the darker face of the reactor with the smaller channels ($70 \times 100\ \mu$m) running perpendicular.

that after the deposition system was cleaned, growth rates were rather small and inhomogeneous growth frequently occurred, a fact which has been noted previously by other research groups.

After results showed that the microchannel reactor/heat exchanger performed differently depending on the amount and the nature of the platinum catalyst, it became evident that further tests were necessary on a system in which the

surface could be directly analyzed. For this reason, a second test reactor/heat exchanger was used, which was not optimized for performance but assembled without diffusion bonding so that the catalyst foils could be removed and analyzed after the experiments. This reactor consists of 5 reaction foils with 39 channels each ($140 \times 200$ $\mu$m) and 4 identical cooling foils, pressed together in a stainless steel frame equipped with metal bolts. Unfortunately, CVD coating was not possible for this system, but rather a sol–gel-type deposition of a porous alumina coating was used (23). Since only a limited number of foils could be placed in the reactor, sufficient heat for the CVD process from the cross-flow channels could not be obtained and the entire test reactor had to be heated in an oven. This results, however, in the alumina also depositing in the entrance section of the reactor and not only in the microstructured channels. Consequently, a sol–gel-type method was selected. In this deposition, the microchannels were filled with an aluminum hydroxide solution (CTA Säureschutz, pH 5.8, 1.70% $Al_2O_3$), which was allowed to slowly dry over a 24-h period, and then calcined at 550°C. The reactivity of the system appears to be similar to that of the CVD process; however, the overall response is substantially slower due to the much higher heat capacity and lower reactive volume. Foils from this setup have been analyzed after the $H_2/O_2$ reaction by X-ray diffraction (XRD), X-ray fluorescence spectroscopy (XRF), scanning electron microscopy (SEM), and energy-dispersive X-ray spectroscopy (EDX).

### 3. *Incorporation of Platinum Catalyst*

Platinum was added to the microchannels by a wet impregnation technique. $H_2[PtCl_6] \cdot 6\ H_2O$ (231 mg) was dissolved in 250 ml of distilled water; this solution was drawn through the reactor five times by applying a gentle vacuum to the exit of the reactor channels. In this manner, the hexachloroplatinic acid solution could be collected and recycled through the reactor. Following the final addition of platinum, the channels were left filled with the solution as to provide a higher amount of the catalyst in the channels after the water had been removed and the platinum salt decomposed. The inlet and outlet to the reactor were cleaned with wet paper swabs before the calcination/reduction step to remove excess platinum which might result in the hydrogen oxidation reaction initiating in these areas.

After the wet impregnation, the reactor was calcined at 570°C and then the catalyst was reduced under $N_2$ and $H_2$ at 350°C. The calcination step was necessary to remove residual organics from the aluminum isopropoxide and to eliminate HCl from the platinum precursor (24). For the calcination, the reactor was heated in a small box furnace under atmospheric conditions with the following heat ramp: heated at 2°C/min to 80°C and held at this temperature for 1 h; heated at 3°C/min to 570°C and held at this temperature for 4 h; and then cooled to room temperature. For the catalyst reduction, the reactor was heated to 350°C by insulating the reactor with ceramic cloth and passing preheated $N_2$ gas (5–7 L/min) through the heat exchanger channels. Subsequently, a 10 : 1 mixture of $N_2$ and $H_2$, 1.0 and 0.1 L/min, respectively, flowed through the $Al_2O_3$/Pt-coated channels for 5 h at the elevated temperature.

Conducting this procedure once, impregnation with Pt followed by calcination and reduction of the reactor, will be referred to in this paper as the low loading of platinum. When the platinum incorporation and calcination/reduction procedure is repeated for a total of three times, the amount of platinum will be designated as a high loading. Unfortunately, one of the limitations of this reactor is that methods to study the surface of the catalyst foils are not available since the surface can only be accessed through the $(140 \times 200)$-$\mu$m channels in this stainless steel block.

To quantitatively determine the total amount of platinum and to measure the particle size in the microchannels, the test reactor/heat exchanger with removable foils in which the alumina was deposited via a sol–gel route (as noted earlier) was used. The Pt precursor for the foils was 240 mg of $H_2[PtCl_6] \cdot 6\ H_2O$ dissolved in 100 ml of distilled water. The impregnation procedure was similar to the one for the CVD alumina, and due to the higher concentration should result in an intermediate value between the low and high loadings used in the standard reactor/heat exchanger.

### 4. *Catalyst Characterization*

Scanning electron microscopy (ATOMIKA/AMRAY 1920 ECO microscope) was used to characterize the $Al_2O_3$ film quality and thickness from the CVD process in a test reactor without the possibility of heat exchanger channels in which individual foils could be removed (25). The imaging of the stainless steel foils was done under simple vacuum and no contrast agents were necessary. The film thickness could be directly measured from the alumina buildup on the flat surface above the channel.

Following the SEM imaging of the foils from the test reactor, physisorption studies confirmed that the introduction of an alumina CVD coating enhances the surface area of the foils. The overall increase in the surface area of the foils produced from the $Al_2O_3$ coating was determined by krypton adsorption using the Sorptomatic 1990 made available from Porotec GmbH.

Energy-dispersive X-ray spectroscopy (Oxford Inca System) studies in conjunction with SEM micrographs (Hitachi S3500-N) measured the distribution of platinum on the alumina surface. Analysis of the entire foil with the EDX revealed the overall distribution for the metal species. X-ray fluorescence spectroscopy (EDAX Eagle II) provided corroboration with elemental analysis. Particle size measurements for these foils were obtained from X-ray diffraction patterns (Stoe STADI P Reflection Diffractometer, Cu $K\alpha$ radiation). Typically, data were collected from 30° to 55° $2\theta$ in 0.02° steps with a count time of 2 s at each point. The divergence slits and receiving slits were 1.2 and 0.8 mm,

respectively. By measurement of the peak width for the Pt reflections, the average platinum particle size could be calculated by the Scherrer equation. This was done before and after the $H_2/O_2$ reaction to establish if the catalyst was sintering.

### 5. *Reactor Operation for the Hydrogen Oxidation Reaction*

Since only the reactor itself contains microchannels with dimensions smaller than the quenching distance for $H_2$, many precautions were taken to safely operate the whole system with hazardous $H_2/O_2$ mixtures. Mass flow regulators were installed in the reactor system to precisely control the amount of the individual gases entering the reactor. A one-way valve was placed before the reactor to prevent exploding gases from entering the stainless steel tubes, shutoff valves, and mass flow controls necessary at this time to mix the gases. An attempt was made to minimize the tubing following the microreactor, thereby restricting the overall volume of gas that could potentially combust.

For the studies with low loadings of Pt, it was necessary to preheat the reactor to initiate the $H_2/O_2$ reaction. This was done by placing the microreactor between two small aluminum blocks equipped with cartridge heaters. The entire unit, microreactor plus block heaters, was wrapped in a ceramic cloth acting as insulation. When the reactor was effectively insulated, trapped heat assisted in raising the reactor temperature rapidly to the final operating temperature, driving the reaction to completion. The external heaters were no longer necessary when more platinum was introduced into the microreactor.

The final part of the reactor system is a cold trap used to monitor the extent to which the $H_2$ was reacted by monitoring the water production. The $H_2O$ leaving the reactor was collected by passing the exiting gas stream through a chilled trap filled with ca. 100 g of dehydrated molecular sieves, kept cold in an ice/salt water bath at $-10^{\circ}$C. Under normal operating conditions, the molecular sieve trap was bypassed until steady state was reached. At steady state, the flow was switched to the trap and the water was collected for a specific amount of time. The rate of water production was determined by differential weighing of the trap before and after the prescribed time period. A comparison of this calculated value for the full conversion of hydrogen with the rate at which the water was collected in the chilled molecular sieve trap gives a value for the extent that the $H_2$ has reacted.

## RESULTS AND DISCUSSION

### 1. *Catalyst Preparation Optimization with Test Reactor*

Prior to coating the microreactor with alumina and introducing the Pt catalyst, the experimental conditions were optimized for a small test reactor with removable micromachined foils and the resulting coatings were evaluated by scanning electron microscopy and krypton adsorption. These techniques were chosen to observe the quality and thickness of the $Al_2O_3$ coating and to quantify the increase in surface area that could be expected (25). Initially, SEM micrographs for the alumina-coated foils showed that a well-coated foil could be prepared as the catalyst support. As seen in Fig. 2, $Al_2O_3$ completely covered the channels of the stainless steel foils; however, the results from the test reactor also showed that to prepare an even alumina coat across the entire set of microchannels, it was necessary to reverse the flow direction for the CVD process and have the $Al(O^iPr)_3$ enter from both sides of the microreactor. With this simple and, nevertheless, necessary step, a fairly uniform coating was obtained.

In SEM experiments, the thickness of the alumina coating was determined in the microchannels; however, this was not done directly in the channel but from a position above the channel which had the same coat thickness. With this flat surface available, a small cut with a scalpel provided a point in the alumina where the thickness could be measured. Presented in Fig. 3 is a SEM micrograph that shows that the thickness of this alumina coat above a microchannel is on the order of 10 $\mu$m, a suitable thickness for a protective coating and one that increased the surface area of the foils by a factor of 100.

The change in the overall surface area was determined by measuring the surface area of the foils with Kr adsorption studies and comparing this value to the total surface created by the system of microchannels between the foils. The surface area measured by Kr adsorption was 0.17 $m^2/g$, a value 100 times higher than the surface area calculated for the channels from simple geometry, including the weight of the individual foils. For the sake of completeness, it should be noted that the original initial intention of the atmospheric CVD deposition of alumina, described in the literature, was for a dense, stable insulator for semiconductor devices that could be used to passivate silicon surfaces (20–22). The purpose of the alumina in the microreactor is to be a protective coat and to act as a catalytic support which raises the overall surface area. Therefore, the CVD conditions which produced the surfaces seen in Figs. 2 and 3 were optimized for a porous alumina coating, not smooth, well-defined surfaces necessary in the semiconductor industry. As observed from the Kr adsorption and SEM results, our aim was achieved and the surface area was increased by 2 orders of magnitude over the geometric surface area.

To measure the concentration of metal species and to assess the effectiveness of distributing the Pt on the alumina surface beginning with the hexachloroplatinic acid, $Pt/Al_2O_3$-coated foils (sol–gel technique) were analyzed by SEM/EDX, XRF, and XRD before and after the $H_2/O_2$

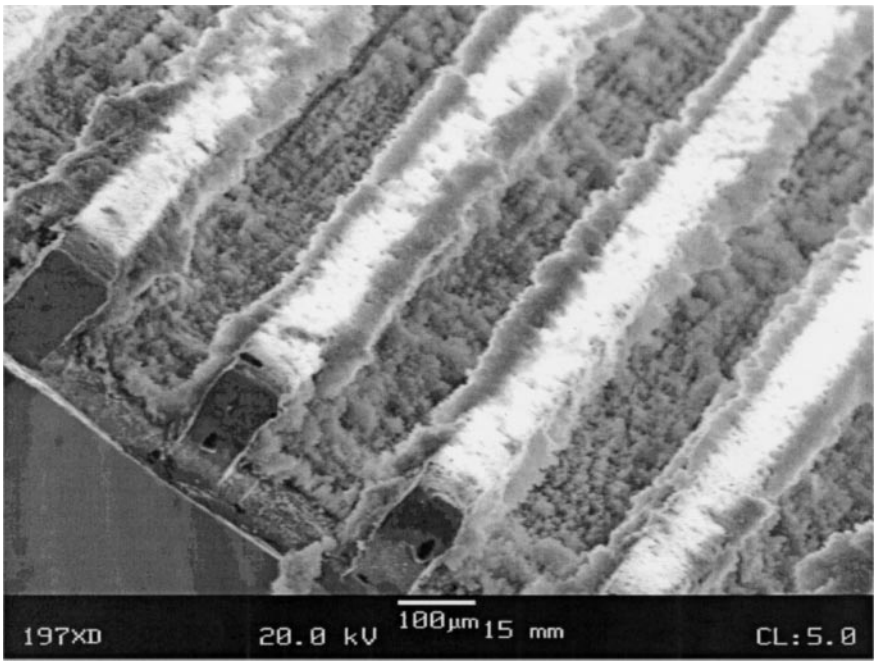


**FIG. 2.** SEM micrograph showing the $Al_2O_3$ coating on an individual microstructured foil. The image was taken at the edge of the foil. Note to obtain a suitable coating, the flow direction for the gaseous mixture containing the $Al(O^iPr)_3$ was reversed following the first deposition step.

reaction. The micrographs with the elemental data provided by the EDX show that platinum is well distributed on the alumina surface (Fig. 4). Shown here is the SEM micrograph with the elemental maps for aluminum and platinum. No obvious changes in the catalyst were observed following the $H_2/O_2$ reaction, indicating that the surface is robust and stable under the reaction conditions. The results also show that the current sol–gel method gives an inhomogeneous

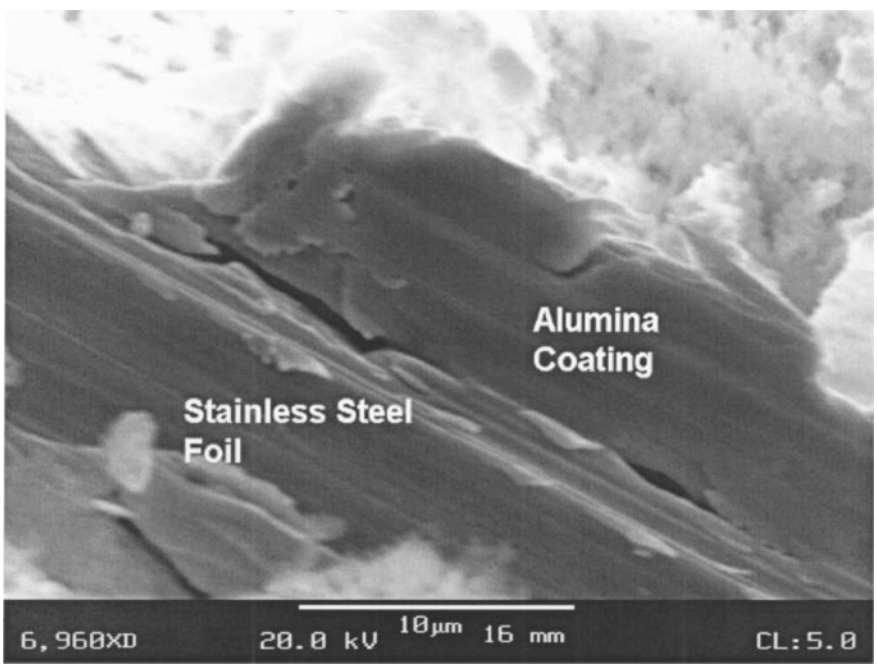


**FIG. 3.** SEM micrograph of the alumina deposited above a microchannel on an adjacent foil. A scalpel has produced a cut through the alumina coating, allowing direct measurement of the film thickness. From the image it appears that the alumina coating is ca. 10-$\mu$m thick. Kr adsorption studies confirm that the alumina coating is porous and increases the surface area of the channels by a factor of 100.

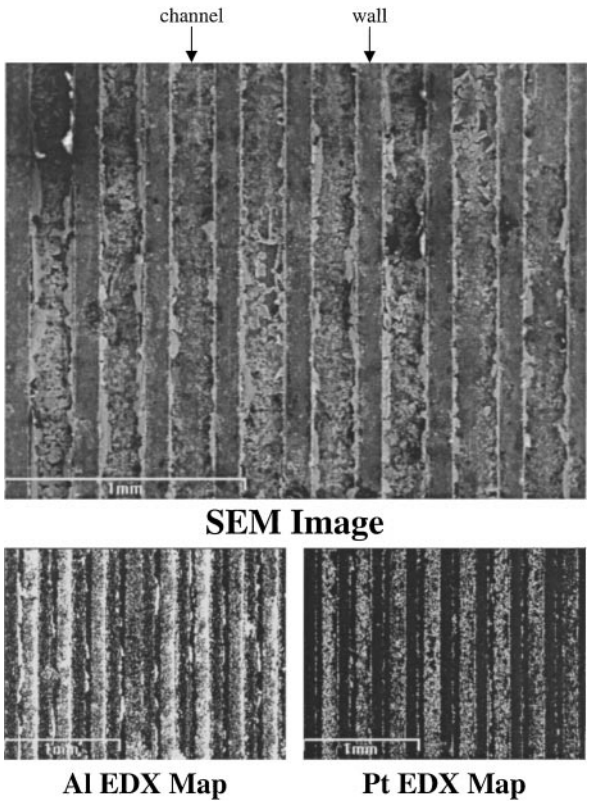


**FIG. 4.** SEM micrograph and EDX measurements showing an elemental map of the surface for one foil that has been coated with $Al_2O_3$ from a sol–gel and impregrated with platinum. From the SEM image, it can be seen that the alumina has coated the channels, but some flaking and inhomogeneities have occurred. Below the micrograph are the EDX elemental maps with the lighter regions in the images representing the respective elements. The lower left image is the Al measurement and reveals a well-dispersed alumina phase in the channels. The lower right image, the elemental map for Pt, shows a nicely distributed metal phase as well. Nearly identical results were found for the foils following the $H_2/O_2$ reaction.

surface and some refinements are necessary for the technique. One can actually expect the catalyst quality in the CVD-coated reactor to be better with respect to homogeneity, as Fig. 2 shows. XRF spectroscopy confirmed that the surface concentration did not change after operation and the ratio of aluminum to platinum on an atomic percentage was 99 : 1.

XRD was used to analyze the Pt particle size. As seen in the XRD patterns, Fig. 5, Pt reflections occur at 39.8° and 46.3° $2\theta$ and reflections for the stainless steel are at 43.7° and 50.8° $2\theta$. For the XRD pattern of the foil following several runs of the $H_2/O_2$ reaction, no substantial differences are observed, even though substantial improvement in the catalytic performance was found. The particle size, as calculated by the Scherrer equation, was $15 \pm 2$ nm and does not change following the $H_2/O_2$ reaction. Therefore, there does not appear to be sintering of the metal catalyst in the system under the experimental conditions reported here which would result in changes to the Pt metal particle size. In addition, no evidence for the formation of a bulk oxide phase could be detected with XRD.

### 2. *Temperature Response for the Reactor/Heat Exchanger with a Low Loading of Platinum*

(All results reported in the following are for the diffusion-bonded reactor unless otherwise stated.) Initial experiments with the microreactor were conducted with a low loading of platinum to test the safety of the $Pt/Al_2O_3$-coated microreactor and to determine if the heat production from the $H_2/O_2$ reaction could be controlled with different fuel mixtures of $O_2$ and $H_2$. For this low amount of platinum, having impregnated the reactor with the hexachloroplatinic acid solution once, additional heaters maintained the reactor temperature at 80°C, a sufficient temperature to initiate the reaction. Displayed in Fig. 6 are plots showing the initial increase in the temperature for the reactant gases exiting the reactor for varying flow rates of $H_2$ and $O_2$ plotted as a function of time. The flow rates of the reactant gases varied from 0.2 and 0.1 L/min to 0.4 and 0.2 L/min for $H_2$ and $O_2$, respectively. In each experiment, the amount of $N_2$ in the system was constant, 1.0 L/min as a diluent for the $H_2/O_2$ mixture and 3.0 L/min for cooling in the second set of microchannels. Note the first temperature points in Fig. 6 do not appear at 80°C because the data have been recorded at the time that the final $H_2$ flow rate was reached. For safety

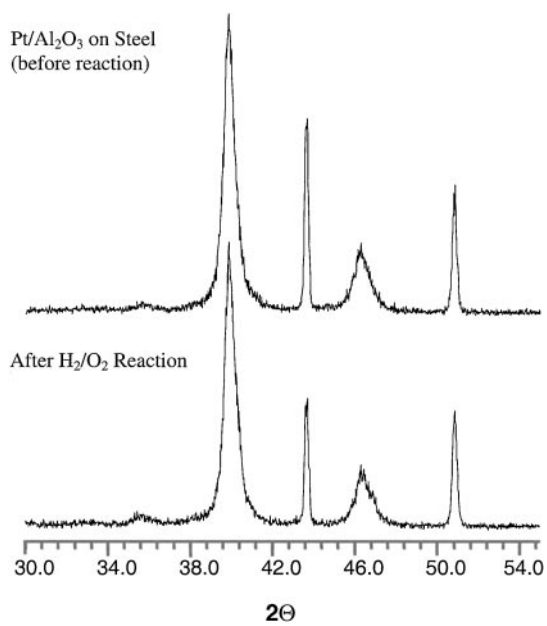


**FIG. 5.** XRD measurements of $Pt/Al_2O_3$-coated foil. Pt reflections occur at 39.8°C and 46.3° $2\theta$, and reflections from the stainless steel are observed at 43.7°C and 50.8° $2\theta$. Reflections from $Al_2O_3$ are not detected, indicating it remains as an amorphous phase. No substantial differences are seen before and after the $H_2/O_2$ reaction and the Pt particle size remains constant at ca. $15 \pm 2$ nm.

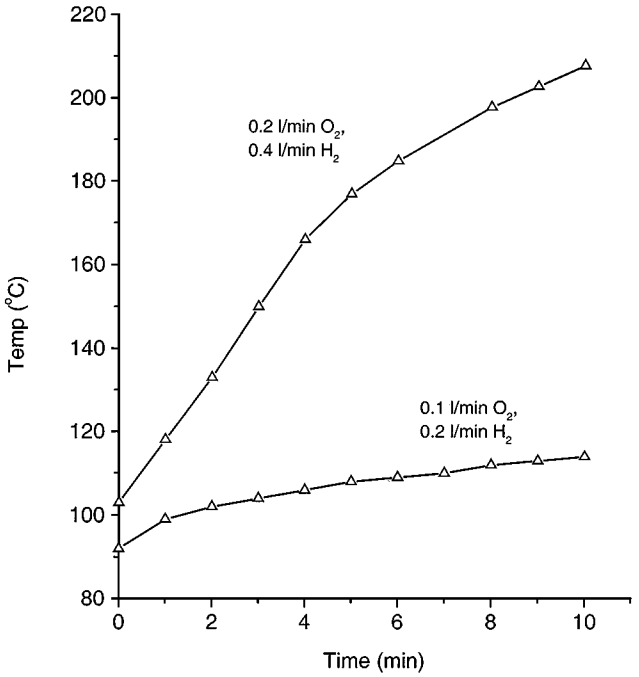


**FIG. 6.** Temperature of the exiting reactant gas plotted as a function of time for various flow rates of $H_2$ and $O_2$. These measurements were made when the microreactor had a low loading of the Pt catalyst. Plotted in this graph is the temperature of the reactant gas stream exiting the reactor as a function of time. Presented alongside the data points are the corresponding amounts of $H_2$ and $O_2$ gas used in each experimental run. The amount of $N_2$ used as a diluent and as a coolant was held constant at 1.0 and 3.0 L/min, respectively. For the lowest flow rates of $H_2$ and $O_2$, there was a small temperature rise in 10 min. As the amount of $H_2$ and $O_2$ in the system increased, a corresponding increase in the heating rate was observed. It was apparent from these results that the composition of the reactant gaseous mixture could control the operating temperature in the microreactor during the $H_2/O_2$ reaction.

reasons, there was no sudden switch to the full $H_2$ flow and the temperature of the reactant gases did increase before the desired $H_2$ flow rate was achieved.

These results in Fig. 6 indicate that the final operating temperature of the reactor can be regulated by the amount and concentration of the $H_2$ and $O_2$ fuel mixture, a first step in demonstrating that a runaway reaction and/or explosion can be avoided. For the lowest concentrations of the reacting gases, 15.4 vol% $H_2$ and 7.7 vol% $O_2$, within a 10-min time span a 25°C increase was measured. However, full conversion had not been achieved at this point. A stoichiometric mixture of 25.0 vol% $H_2$ and 12.5 vol% $O_2$ provided for a 110°C temperature rise in 10 min to approximately 220°C, at which point the hydrogen was fully converted to water; see below. The temperature of the $N_2$ cooling gas was roughly 20°C warmer than the temperature for the reaction gases. This implies that a hot spot in the front of the reactor exists and the cross-flow design of the reactor leads to some cooling of the reactant gases (26). The outcome is the reaction initiates without exploding and the heating rate can be controlled by the concentrations of the reacting gases.

It was not only important to demonstrate in this study that the microreactor operates safely but also that the exiting gases were outside the explosion regime for $H_2$ and that 100% of the $H_2$ had been converted to water. For this reason, the total amount of water was measured and the conversion calculated as described in the Experimental section. In one such experiment, the following flow rates were tested: 0.4 L/min $H_2$, 0.2 L/min $O_2$, 1.0 L/min $N_2$ as the diluent, and 7.0 L/min $N_2$ as the coolant. For a freshly prepared platinum catalyst, with a final reactor at a steady-state temperature of 219°C, all of the hydrogen was converted to $H_2O$ as measured by the water collected in the chilled molecular sieve trap. $H_2O$ (9.9 g) was produced in 30 min at a rate of 0.33 g/min. From the flow rate of 0.4 L/min, and assuming ideal gas behavior, the approximate rate at which water would be produced with 100% conversion of the hydrogen is 0.32 g/min. Small errors might be present, namely, water that is present in the process gases or water that is left in the transfer tube between the reactor and trap; however, we expect these to be small and on the order of $\pm 1\%$. Therefore, within the errors of this measurement, it appears that the microreactor system converts 100% of the $H_2$ gas to water at nominal temperatures, resulting in an exit gas depleted in hydrogen and out of the explosive regime. Additionally, a simple heat balance of the system reveals that 20 W is necessary to heat the gases in the system. With 72 W of power possible from the heat of the reaction with this flow rate of $H_2$, approximately 70% of the heat is lost. It is anticipated that better insulation of the system will minimize these losses.

The reactor was also successfully operated without diluent gas, confirming the inherent safety associated with the microreactor. A 1:1 mixture of $H_2$ and $O_2$, 0.8 L/min of each and clearly in the middle of the explosion regime for hydrogen gas, was flowed through the preheated microreactor. With these reactor conditions, there was a rapid increase in temperature without any difficulties. By the time the flow rate of $H_2$ reached 0.8 L/min, the reactor temperature had exceeded 300°C, roughly a 5-min time span. The reaction was stopped before, however, a steady state could be reached, in case a hot spot existed in the entrance to the reactor that was hotter than the temperature to ignite the homogeneous reaction, to avoid explosions in the mixing zone. With the experimental setup, only 15 L/min of $N_2$ gas was available as a coolant and this did not provide a sufficient amount of cooling. This example, however, still demonstrates the ability of the microreactor to manage dangerous mixtures of gases.

Although the microreactor/heat exchanger normally operates without problems as the $H_2$ oxidizes to $H_2O$ over the Pt catalyst, on occasion there are some times of instability that were observed when the reactor would not reach a

steady-state temperature. In initial trial experiments, the reactor was coated with alumina, impregnated with platinum, tested in the reaction, and cleaned several times. Usually, the reactor performance proved to be reproducible; however, when instabilities occurred with one coating, several small explosions were observed. The only indications that they occurred were a quick popping sound; the gases briefly ceased to flow through the system, and oil from the bubbler (installed at the gas exit and used as a visual flow indicator) was drawn back toward the reactor at which point the reaction had stopped and the temperature of the reactor dropped to the original temperature determined by the heating blocks. After dry gases passed through the reactor, the reaction would begin again. The reason why this particular coating led to instabilities could not be determined since the reactor cannot be disassembled. Obviously, the reaction did not initiate in the reactor channels but at the inlet or outlet of the system, perhaps due to an enrichment of platinum in one of these areas, resulting from an error during the catalyst incorporation. The key point is, however, that the explosions were relatively harmless and might have gone unnoticed without assistance from the bubbler.

More stringent tests were done at the Fraunhofer Institute of Chemical Technology (FhG-ICT) where the microreactor was tested for its ability to act as a flame resistor. In these experiments, a vessel of hydrogen was attached to one side of the reactor and a vessel of oxygen to the other and the gases were allowed to diffuse between the two sides through the reactor. An explosion was ignited on one side of the reactor, but it could not pass through the microchannels to the other side, demonstrating the effectiveness of the microreactor to stop the propagation of explosions without damaging the thin stainless steel plates (27). These two examples of explosions involving the microreactor/heat exchanger, from research presented here and the results from the work at FhG-ICT, confirm that during such events a high level of safety is still maintained while in larger reactors such occurrences could be catastrophic.

### 3. *Temperature Response for the Reactor/Heat Exchanger with a High Loading of Platinum*

Very promising results for the $Pt/Al_2O_3$-coated microreactor were acquired after more platinum was incorporated. Namely, with repetition of the Pt impregnation and calcination/reduction step for a total of three times, the reaction initiated at room temperature and external heaters were no longer necessary. Shown in Fig. 7 are similar data as presented earlier, the temperature of the reactant gases exiting the reactor plotted as a function of time. For this series of experiments the flow rates of the $N_2$ diluent, $O_2$, and $H_2$ are kept constant at 1.0, 0.2, and 0.4 L/min, respectively, with three runs having the $N_2$ cooling gas set at 4.0, 5.0, and 7.0 L/min. The quantity of $N_2$ cooling gas was adjusted to show that the overall operating temperature can again

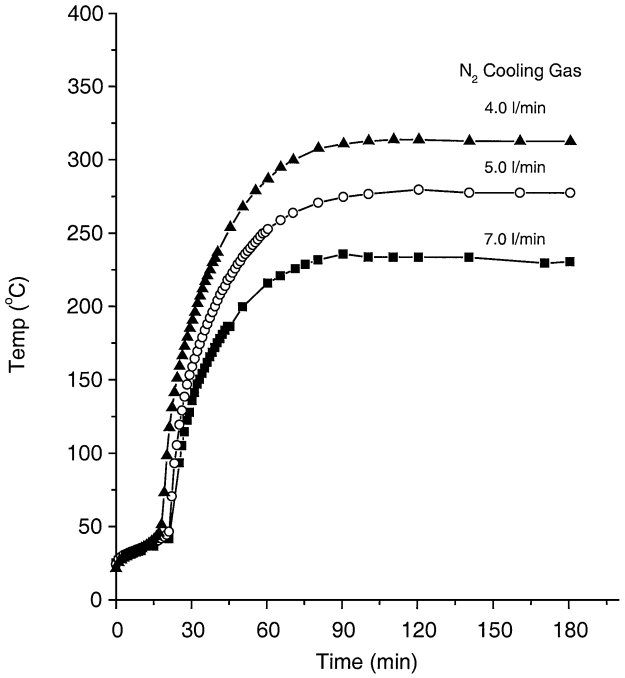


**FIG. 7.** Temperature response results for the microreactor with a high loading of platinum. Plotted in this graph is the temperature of the reactant gas stream exiting the reactor as a function of time. For each experiment the flow rates of $H_2$ and $O_2$ were 0.4 and 0.2 L/min, respectively, and the amount of $N_2$ as a diluent was 1.0 L/min. For the different experimental runs the amount of $N_2$ cooling gas was varied between 4.0 and 7.0 L/min, as shown in the plot. As with the previous results in Fig. 4, the data reveal that the final operating temperature of the reactor again can be controlled, in this case with the $N_2$ cooling gas. For these results, however, no heating from the external heaters was necessary and the reaction initiated at room temperature. The temperature of the cooling gases was ca. 20°C higher than the reaction gases.

be controlled. With the microreactor initially at room temperature, in all cases the temperature of the reactor slowly increased to 50°C, at which point the reaction ignited and heated the reactor system to the final operating temperatures. These temperatures were approximately 315, 280, and 230°C for the respective $N_2$ cooling gas rates of 4.0, 5.0, and 7.0 L/min. It was found that the exiting cooling gas temperature again was approximately 20°C hotter than the exiting reaction gases. Additionally, at these final operating temperatures there was in each experiment 100% conversion of the $H_2$ to $H_2O$ and simple heat balances show that, of the 72 W of power possible, approximately 25 W was used to heat the reactant and coolant gases. These encouraging results differ from the earlier findings with the lower amount of Pt incorporated into the microreactor in that the reaction clearly initiates at room temperature, eliminating the need for external heaters, and the reactor functioned reliably without the instabilities experienced previously. It should also be mentioned that the composition of the reactant gases for 1.0 L/min $N_2$ and 0.2 L/min $O_2$, excluding the $H_2$, is roughly the same as dry air, 83% $N_2$ and 17% $O_2$ by

volume. Thus, air is a potential carrier gas for the hydrogen oxidation reaction, an attractive proposal for the use of this catalytic heater in the development of fuel cell systems.

To test the effect of higher flow rates on the final steady state, experiments with higher flow rates in the reactant stream were performed. The overall heat balance was maintained by keeping the amount of nitrogen gas constant in the system. The flow rate for the diluent gas was increased and this was compensated for by less coolant (reaction conditions: 0.4 L/min $H_2$, 0.2 L/min $O_2$, 2.0 L/min $N_2$ as the diluent, and 3.0 L/min $N_2$ as the coolant). In this case, the ignition and steady-state operating temperatures did not change; however, under more dilute conditions the induction period was longer. This suggests the hot zone in the reactor is not greatly affected by the flow rates for the gases, but this will become a more critical issue if the coolant is changed to a fluid with a higher heat capacity (26).

For the microreactor, there was a dramatic improvement in the induction period prior to the ignition of the reaction with each successive experimental run. As shown in Fig. 8 (reaction conditions: 0.4 L/min $H_2$, 0.2 L/min $O_2$, 1.0 L/min $N_2$ as the diluent, and 4.0 L/min $N_2$ as the coolant), the first reactor test required in excess of 30 min to reach the ignition temperature. The second set of data on this plot represents the results for the fifth reactor run. For this trial with the same reactor conditions, the induction period decreased to approximately 5 min, igniting shortly after the hydrogen reached the full flow rate. Note these experiments differ slightly from those presented in Fig. 7. In the previous experiments, the heating blocks were still in place; however, they were not used. They were removed prior to collecting the data shown in Fig. 8 because they were acting as heat sinks, and as a result the final operating temperature for the reactor increased to 375°C. Apparently, the calcination/reduction process does not yield the optimal catalyst and changes during the course of the $H_2/O_2$ reaction produce a more active catalyst with a shorter induction period. To confirm this, the reduction/calcination procedure was repeated and the length of the induction period was again measured with the same reactor conditions as above. The results from this experiment, along with the original data, are presented in Fig. 9. Immediately following this second calcination and reduction of the catalyst, the induction period was greater than 90 min, entirely too long for the application in mind for this microreactor. However, in the second run following the calcination/reduction the induction period decreased once again to under 10 min, and

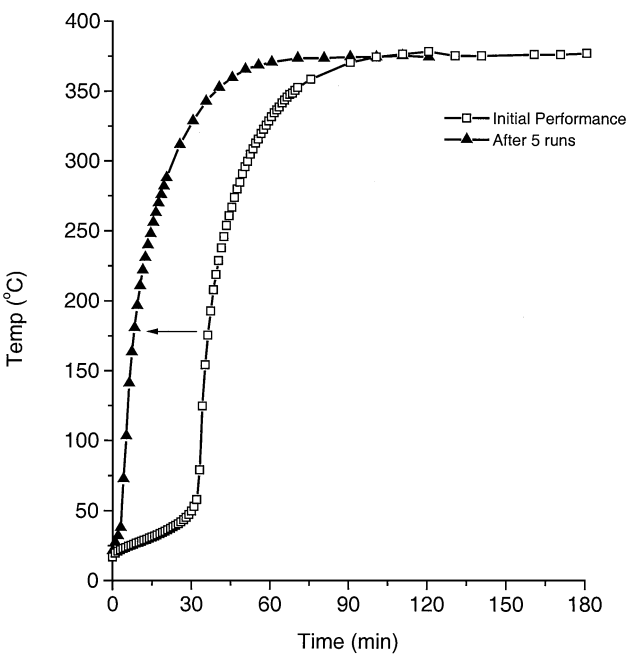


**FIG. 8.** Temperature response for the microreactor after five experimental runs following the removal of the heating blocks. Plotted is the same data from Fig. 8 with the $N_2$ cooling gas at 4.0 L/min (-□-) and the results for the fifth trial with the reactor under the same operating conditions (-▲-). Observed is a dramatic decrease in the induction period before the reaction ignites. Initially, the time needed to reach the ignition temperature of ca. 50°C was over 30 min. On the fifth run, it was less than 5 min.

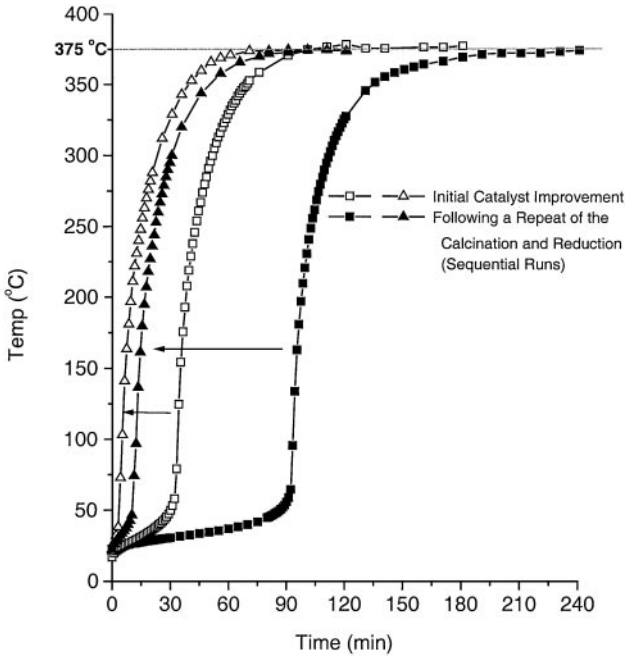


**FIG. 9.** Temperature response for the first and second experimental runs of the microreactor following a second calcination/reduction period. Plotted in this figure is again the temperature of the exiting reactant gas stream. The first run after the second calcination/reduction procedure (shown in -■-) had an induction period that was over 90 min. In the sequential experiment (-▲-), the time before the $H_2/O_2$ reaction ignited reduced to under 10 min and further improvements were observed with each subsequent run. With this data are the results shown in Fig. 6 (-△- and -□-) to clearly demonstrate the drastic differences in the microreactor performance following the calcination and reduction step. This disparity in performance will be the focus of our future research efforts.

this continued to improve in subsequent runs. Thus, it appears as if the $H_2/O_2$ reaction generates a catalyst with a shorter induction period than can be prepared by simple hydrogen reduction of the metal, an occurrence observed earlier with hydrogen oxidation on Pt and in other systems such as the combustion of methane on a $Pd/SiO_2$ catalyst, for example (28–30).

There have been several proposals to explain this improvement in Pt catalysts after exposure to the hydrogen oxidation reaction. One explanation is that an oxide layer dramatically alters the catalytic activity of the Pt catalyst (28, 29). From experiments on oxidized and reduced Pt surfaces, Gentry *et al.* determined that platinum metal oxidized in air had an increased catalytic activity toward hydrogen oxidation (28). These results suggested that weakly absorbed hydrogen and strongly absorbed oxygen reacted with a much higher reaction rate than those for $H_2$ and $O_2$ on a reduced platinum surface. Hanson and Boudart later reported that in an excess of $O_2$ there is a corrosive chemisorption of oxygen which erases structural features of the catalyst, leading to a markedly changed surface (29). Additional studies of Pt on $Al_2O_3$ supports have shown that structural changes in the platinum at elevated temperatures, sintering, for example, also affect the availability and performance of the catalyst (31–35). The XRD and XRF results do not detect any specific changes that are readily identified, such as changes in the Pt surface concentration or morphology. It thus appears that more subtle and microscopic effects, such as the formation of a thin surface or subsurface oxide layer, which cannot be detected in our XRD experiments, could be responsible for the improved performance of the catalysts after several runs. Future directions for this research will continue to focus on identifying what specific events occur during the course of the $H_2/O_2$ reaction in the reactor and how these effects influence the overall performance. The strategy will be to continue to utilize the reactor with removable foils, allowing direct analysis of the platinum and alumina support after preparing the catalyst with surface analytical techniques.

## CONCLUSIONS

In this investigation, the use of a microstructured reactor/heat exchanger was shown to be a capable, safe option for conducting catalytic tests with mixtures of explosive gases. The combination of small microchannels below the quenching distance for $H_2$ gas and the efficient heat removal through the heat exchanger side allowed dangerous mixtures of $H_2$ and $O_2$ to be mixed and reacted safely in the $Pt/Al_2O_3$-coated microchannels. With the results presented, it is clear that the operating temperature can be controlled through the composition and flow rates of the various gas components and coolants, key to implementing microreactors in current chemical processes. In such a way, runaway reactions and explosions can be avoided. Remarkably, through repeated use of the microreactor, a dramatic improvement in the catalyst performance was discovered with a sharp reduction in the induction period necessary to ignite the reaction from room temperature which cannot be explained by sintering or a change in particle size for the Pt. Future research with this system will continue with the test reactor in which the surface of the foils can be analyzed. In this way, direct studies of the catalyst will identify the specific modifications that led to the increased performance and identify specific areas where progress can be made. Although a static micromixer was not used in this work, micromixers add a further level of improvement to the reactor design and will also be incorporated in future studies (36). Micromixers have the advantage that gases do not mix in large volumes and pass through the reactor. Instead, the gases or liquids pass through a series of micron-sized channels. Upon exiting these channels, the microstreams are separated by ca. 100 $\mu$m and mix rapidly over very short distances. Once again explosive gases are restricted to small spaces in the static micromixer which minimize the explosion risk. This additional level of safety will aid in promoting the use of microreactors as valuable additions to laboratories, chemical plants, and other applications such as fuel cell systems, the primary goal of this research.

## ACKNOWLEDGMENTS

The authors would like to thank the Alexander von Humboldt Foundation for financial assistance (M.T.J.), the Research Center Karlsruhe which initiated and sponsored this project, and C. Weidenthaler (XRD), H.-J. Bongard (SEM), and J. Rust (XRF) for their experimental assistance.

## REFERENCES

1. Bier, W., Keller, W., Linder, G., Seidel, D., and Schubert, K., *in* "DSC-19, Microstructures, Sensors and Actuators" (D. Cho *et al.*, Eds.). The American Society of Mechanical Engineers, Book No. G00527, 1990.
2. Papers from the Workshop on Microsystem Technology for Chemical and Biological Microreactors, DECHEMA Monograph, Vol. 132. VCH, New York, 1995.
3. "Proceedings from the 2nd International Conference on Microreaction Technology, New Orleans, March 9–12, 1998."
4. Ehrfeld, W., Hessel, V., Möbius, H., Richter, Th., and Russow, K., *in* "Microsystem Technology for Chemical and Biological Microreactors," DECHEMA Monograph, Vol. 132. VCH, New York, 1995.
5. Jäckel, K.-P., *in* "Microsystem Technology for Chemical and Biological Microreactors," DECHEMA Monograph, Vol. 132. VCH, New York, 1995.
6. Lerou, J. J., Harold, M. P., Ryley, J., Ashmead, J., O'Brien, T. C., Johnson, M., Perrotto, J., Blaisdell, C. T., Rensi, T. A., and Nyquist, N., *in* "Microsystem Technology for Chemical and Biological Microreactors," DECHEMA Monograph, Vol. 132. VCH, New York, 1995.
7. Rinard, I., *in* "Proceedings from the 2nd International Conference on Microreaction Technology, New Orleans, March 9–12, 1998."
8. Kursawe, A., Dietzsch, E., Kah, S., Hönicke, D., Fichtner, M., Schubert, K., and Wießmeier, G., *in* "Proceedings from the 3rd International Conference on Microreaction Technology, Frankfurt, Germany, April 18–21, 1999."

9. Hönicke, D., and Wießmeier, G., *in* "Microsystem Technology for Chemical and Biological Microreactors," DECHEMA Monograph, Vol. 132. VCH, New York, 1995.
10. Srinivasan, R., Hsing, I.-M., Berger, P. E., Jensen, K. F., Firebaugh, S. L., Schmidt, M. A., Harold, M. P., Lerou, J. J., and Ryley, J. F., *AIChE J.* **43**, 3059 (1997).
11. Tonkovich, A. L. Y., Zilka, J. L., Powell, M. R., and Call, C. J., *in* "Proceedings from the 2nd International Conference on Microreaction Technology, New Orleans, March 9–12, 1998."
12. Hagendorf, U., Janicke, M., Schüth, F., Schubert, K., and Fichtner, M., *in* "Proceedings from the 2nd International Conference on Microreaction Technology, New Orleans, March 9–12, 1998."
13. Tonkovich, A. L. Y., Jimenez, D. M., Zilka, J. L., LaMont, M. J., Wang, Y., and Wegeng, R. S., *in* "Proceedings from the 2nd International Conference on Microreaction Technology, New Orleans, March 9–12, 1998."
14. Weast, R. C. (Ed.), "CRC Handbook of Chemistry and Physics," 6th ed., p. D-124. CRC Press, Inc., Boca Raton, FL, 1985.
15. This value was taken from an article by Gerhard, F., *in* "Ullmann's Encyclopedia of Industrial Chemistry," 5th ed., Vol. A18. VCH Publishers, New York, 1991. For detailed explanations and calculations, see for example Bartknecht, W., "Explosionen-Ablauf und Schutzmaßnahmen." Springer-Verlag, Berlin, 1980; Drell, I. L., and Belles, F. E., "Survey of Hydrogen Combustion Properties," NACA Report 1383, 1958; Simon, D. M., Belles, F. E., and Spakowski, A. E., "Fourth Symposium (International) on Combustion," pp. 126–138. The Reinhold Pub. Corp., Baltimore, 1953; Lewis, B., and von Elbe, G., "Combustion, Flames, and Explosions of Gases." Academic Press Inc., New York, 1951.
16. Berlin, B., *Science* **279**, 330 (1998).
17. Peters, R., Düsterwald, H. G., Höhlein, B., Meusinger, J., and Stimming, U., "Scouting Study about the Use of Microreactors for Gas Supply in a PEM Fuel Cell System for Traction," preprint.
18. Düsterwald, H. G., Höhlein, B., Kraut, H., Meusinger, J., Peters, R., and Stimming, U., *Chem. Eng. Technol.* **20**, 617 (1997).
19. Schaller, Th., Bier, W., Linder, G., and Schubert, K., "Mechanische Mikrotechnik für Abformwerkzeuge und Kleinserien," Report No. FZKA 5670, pp. 45–50. Forschungszentrum Karlsruhe, Karlsruhe, Germany, 1995.
20. Saraie, J., Kwon, K., and Yodogawa, Y., *J. Electrochem. Soc.* **132**, 890 (1985).
21. Saraie, J., Ono, K., and Takeuchi, S., *J. Electrochem. Soc.* **136**, 3139 (1989).
22. Aboaf, J. A., *J. Electrochem. Soc.* **114**, 948 (1967).
23. See for example Narula, C. K., "Alumina Oxide Catalyst Supports from Alumina Sols" U.S. Patent 5,210,062, 1993 and the references therein.
24. Barbier, J., Bahloul, D., and Marecot, P., *J. Catal.* **137**, 377 (1992).
25. Kestenbaum, H., Diplomarbeit, Johannes Wolfgang Goethe Universität, Institut für Anorganische Chemie, Frankfurt, Germany, Dec. 1997.
26. Janicke, M., Holzwarth, A., Fichtner, M., Schubert, K., and Schüth, F., "A Microstructured Catalytic Reactor/Heat Exchanger for the Controlled Catalytic Reaction between $H_2$ and $O_2$" *Stud. Surf. Sci. Catal.*, in press.
27. Internal Report, Fraunhofer Institut für Chemische Technologie, July 1996.
28. Gentry, S. J., Firth, J. G., and Jones, A., *J. Chem. Soc. Faraday Trans.* **70**, 600 (1974).
29. Hanson, F. V., and Boudart, M., *J. Catal.* **53**, 56 (1978).
30. Pecchi, G., Reyes, P., Concha, I., and Fierro, J. L. G., *J. Catal.* **179**, 309 (1998).
31. Fiedorow, R. M. J., and Wanke, S. E., *J. Catal.* **43**, 34 (1976).
32. Dautzenberg, F. M., and Wolters, H. B. M., *J. Catal.* **51**, 26 (1978).
33. Den Otter, G. J., and Dautzenberg, F. M., *J. Catal.* **53**, 116 (1978).
34. Straguzzi, G. I., Aduriz, H. R., and Gigola, C. E., *J. Catal.* **66**, 171 (1980).
35. Sushumna, I., and Ruckenstein, E., *J. Catal.* **109**, 433 (1988).
36. Schubert, K., Bier, W., Brandner, J., Fichtner, M., Franz, C., and Linder, G., "Proceedings from the 2nd International Conference on Microreaction Technology, New Orleans, March 9–12, 1998."